SPS/ABM/JB/Tech.Note/77-9 10 October 1977

AIR ČERENKOV DETECTOR

J. Bosser, J. Dieperink, J. Mann, W. Okx*)

1. Introduction

A detector using the principle of light yield by Čerenkov effect is now in use in the SPS WEXTR extracted proton beam line. It is intended to give a visual display of the slow and fast-slow modes of extraction. The output of the resulting signal has a bandwidth of about 10 MHz. However, as will be explained later, some precautions had to be taken for the safe use of this detector.

2. Principle

2.1 Principle of Čerenkov radiation

Numerous reports deal with this subject in extension (see ref. 1 for more details); in the following we shall limit ourselves to a few formulae only necessary to ensure comprehension.

An electromagnetic wave is associated with a charged particle in movement. If this particle of constant velocity 'v' passes through a transparent medium with a refractive index 'n', it creates an electromagnetic wave with a continuous spectrum in case where $v > \frac{c}{n}$ (c being the velocity of light in vacuum). This is the so-called Čerenkov radiation.

---

*) Student from Hogere Technische School 's-Gravenhage, Holland.

Tamm and Frank developed a classical theory where it appears that the radiated light is emitted along a conical wavefront. The angle 'θ' of emission is expressed by (see fig. 1):

$$\cos \theta = \frac{1}{\beta n} \qquad (\beta = \frac{v}{c})$$

The number 'N' of photons emitted per unit of length 'L' and per particle is given by

$$\frac{dN}{dL} = 2\pi\alpha Z^2 \int_{\lambda_1}^{\lambda_2} \left(1 - \frac{1}{[\beta n(\lambda)]^2}\right) \frac{d\lambda}{\lambda^2}$$

where

λ is the wavelength

α is the fine structure constant ($\alpha \simeq \frac{1}{137}$)

Z.e is the charge of the particle

λ_1, λ_2 being the lower and upper wavelength of the detected radiation.

The yield of light (number of photons) is proportional to the number of traversing protons in the medium.

2.2 Principle of the detector (fig 2 and photo 1)

The main parts of the detector are:

- A tank associated with a vacuum system. During normal operation the tank is full of air at normal atmospheric pressure. It is closed at both ends to ensure that no external parasitic light enters and to make the decrease of pressure possible when needed.
- A mirror
- An optical window
- A light collector
- A photo-multiplier
- Cables, power supplies
- Some special electronic circuits.

The proton beam at 200 GeV passing through the tank produces a Čerenkov radiation in the air, as explained in part 2.1. The radiation is deflected by a mirror in order to reach the photo-cathode of a photo-multiplier (P-M). After amplification by the P-M, the signal is transmitted by means of a high performance cable and displayed at distance on a scope.

At 200 GeV and at normal pressure conditions, the emission angle is about 2^{o}. The angle of the mirror is 45^{o} with respect to optical axis.

Between the mirror and the P-M a cone has been provided in order to move the P-M away from a location of high radioactivity level.

Since the light is emitted in a cone, it was possible to insert a diaphragm between beam entrance and mirror in order to reduce the background light due to scintillation or ionisation.

3. Design

Figure 3 gives an overall view of the control of the detector.

3.1 Physical parameters

The radiator presently in use is air. Table 1 gives the refractive index for different gases. In our case the dependence of the refractive index on pressure 'P' is approximately

$$(n - 1) = (n_o - 1)P$$

where n_o is the refractive index of the gas at a defined wavelength and temperature and at the pressure of one atmosphere.

This led us to a 'threshold pressure P_{th}' below which no Čerenkov light is induced.

For air and at 200 GeV:

$$\cos\Theta = \frac{1}{\beta n_{th}} = 1 \quad \Rightarrow n_{th} = 1.000010896 = \frac{1}{\beta}$$

$$P_{th} = \frac{n_{th} - 1}{n_o - 1} = 0{,}037218 \text{ atm (or 28.2 Torr).}$$

Angle 'Θ' allows us to define the minimum mirror and diaphragm size which are 44 and 30 mm diameter respectively (including the safety for position beam jitter).

3.2 Mechanical parameters

The tank is the same as that used for the present SPS Beam Television Monitors (BTV).

To make the changing of internal pressure possible, the tank is closed at each end by two beam windows made of 0.2 mm thick aluminium foils.

The plane mirror is a two-sided aluminised mylar. It is put in the beam in place of the BTV screens with the usual mechanism.

Experience has shown that after continuous irradiation of the mirror by the beam during a period of about 2 weeks, the aluminium has been evaporated and holes have been burnt in the supporting mylar. To overcome this degradation a hole of 10 mm diameter has been drilled in the centre of the mirror.

As can be seen in fig. 3, the radiated light leaves the tank through a glass window. To match the difference in diameter between the glass window and the photo-cathode, a conical guide has been implemented.*) This guide directs the radiated photons from the tank to the photo-cathode but also removes the P-M away from the beam thus reducing radiation damage.

The detector tank is equipped with a remotely controlled vacuum system. Except during operational periods, the tank is emptied in order to reduce the emittance blow-up of the beam.

---

*) the internal part of this cone is made reflective

3.3 Electrical parameters

The P-M in use is of the type XP2020 with its normal CERN power supply. The voltages applied to the cathode, dynodes and anode are remotely controlled.

Some difficulties appeared with respect to the different extraction modes of the SPS. For the same amount of extracted protons the fast extraction will generate 43.000 (1 sec/23 μs) times more photons than the slow extraction. The detector is dedicated to the slow extraction monitoring. In consequence a correct voltage setting for slow extraction will lead to a destructive anode current when fast extraction occurs.

To overcome this difficulty a simple gain switching unit has been developed. This applies the right voltage to the P-M during the slow extraction period and reduces the voltage (and in this way the gain of the P-M) at any other time of the cycle. The switching unit is controlled by the usual SPS timing modules. The two voltage levels are remotely controlled.

4. Results

4.1 Theoretical values expected

Appendix 1 gives few mathematical results where it appears finally a yield of 0.20328 photo-electrons per extracted proton.

If, for example, we consider $5 \cdot 10^{12}$ extracted protons in one second, this gives

$$0.20328 \times 1.6 \times 10^{-19} \times 5 \times 10^{12} = 162.63 \text{ nA}$$ photo-cathode current.

In the case of 1000 V between cathode and anode the photo-multiplier gain is expected to be 10^4 (ref. 4). As a result the theoretical output current will be about 16 mA and the mean output voltage 80 mV into 50 Ω.

4.2 Experimental results

(a) Linearity

In order to verify the linearity of the detector the output of the Čerenkov detector is integrated and normalised by the corresponding integrated signal of the BSPV 6102 (split foil secondary emission monitor).

Figure 4 gives a plot of this result. It appears that the monitor is linear in the range of 800 V to 1120 V. However, for higher voltages the non-linearity may be due to the current limitation of the power supply.

In any case, it appears that a working voltage of the order of 1000 V is quite efficient.

(b) Analysis of the results

- Photo 2 gives an overall picture of the output signal with a constant voltage of 800 V. The scope is triggered with the injection event. Slow and fast-extracted signals appear clearly.

- Photo 3 shows the influence of the voltage reduction during fast extraction. During slow extraction, the high voltage is set to -1000 V at a beam intensity of about $5 \cdot 10^{12}$ in order to compare the agreement of theoretical and practical results.

- Photos 4 and 5 give a detailed picture of the slow-extracted spill. The 'gap' appears clearly every 23 μs.

- Photos 6 and 7 give a picture of the 'fast slow' spill.

- Photo 8 shows the resulting signal of a fast extraction.

- Photo 9 gives a detailed analysis of an extraction where it appears that a frequency up to 10 MHz can be observed.

5. Conclusions and future improvements

This detector seems to give the expected results. The major problem remaining is to find a safe solution for the high voltage switching, as explained in para. 3.3.

Some improvements can be achieved such as:

- The implementation of a remotely controlled diaphragm in front of the photo-cathode,
- The studies of the light yield by various gases used as radiators,
- The use of light guides in order to prevent the P-M from too high radiation doses,

- The development of a self-ranging gain circuit which determines, after a few cycles of operation, an output level normalised to the beam average intensity,
- Integration of the detector into the vacuum system,
- A non-deteriorating mirror.

Acknowledgements

This work is the result of several discussions with L. Burnod. The mechanical part has been realized by J. Camas and J. Donnier. We thank H. Verveij for the help and recommendations given during this project.

Estimation of the number of photoelectrons

In the Tamm-Frank theory the number of emitted Čerenkov photons per passage of a charged particle and per detector length is given by:

$$\frac{dN}{dL} = 2\pi\alpha Z^2 \int_{\lambda_1}^{\lambda_2} \left(1 - \frac{1}{\beta^2 n^2}\right) \frac{d\lambda}{\lambda^2}$$

The equation shows that most of the Čerenkov light appears at small values of λ.

In the present case the gas will be homogeneously distributed along the detector, so the equation becomes:

$$N = 2\pi\alpha Z^2 L \int_{\lambda_1}^{\lambda_2} \left(1 - \frac{1}{\beta^2 n^2}\right) \frac{d\lambda}{\lambda^2}$$

By using the relation $\cos\Theta = \frac{1}{\beta n(\lambda)}$ one can write

$$N = 2\pi\alpha L Z^2 \int_{\lambda_1}^{\lambda_2} \sin^2\Theta \, \frac{d\lambda}{\lambda^2}$$

in which Θ is a function of λ. This function has been investigated for air and was found to be in good approximation constant over the range 390 - 600 nm, which is the range in which the detector is sensitive (see table 2).

Thus the photon yield per proton is defined by

$$N = 2\pi\alpha L Z^2 \sin^2\Theta \left[\frac{1}{\lambda}\right]_{\lambda_2}^{\lambda_1} \text{ photon}/\text{proton}$$

which, in the case of air, can be written as

$$N = 2\pi \frac{1}{137} 0.55 \sin^2 1.35 \left[\frac{10^9}{390} - \frac{10^9}{600}\right] = 12.75 .$$

The relation between incident photons and resulting photoelectrons in the P-M is called quantum efficiency and is stated by the manufacturer[4]:

$$QE = N_{kr} \frac{1.24}{\lambda} \left[\text{photoelectr.}/\text{photon}\right]$$

in which N_{kr} is a typical photo-cathode function as shown in the graph of fig. 5a. In order to obtain the total number of photoelectrons due to a photon in a certain range, let us write

$$dQE = 1.24\, N_{kr} \frac{-1}{\lambda^2} d\lambda + \frac{1.24}{\lambda} d\, N_{kr}$$

Then the total range is split up into smaller ranges in which the cathode radiant sensitivity N_{kr} is approximated to be constant, so

$$\sum_{\text{no ranges}} dQE = \sum_{I=\text{ no ranges}} -1.24 \frac{N_{krI}}{\lambda^2} d\lambda$$

and the total quantum efficiency is given by

$$QE_{tot} = \sum_{I=1}^{4} \left| \int_{\lambda_1}^{\lambda_2} -1.24 \frac{K_{krI}}{\lambda^2} d\lambda \right|$$

$$= \sum_{I=1}^{4} \left| 1.24 \cdot N_{krI} \int_{\lambda_1}^{\lambda_2} -\frac{d\lambda}{\lambda^2} \right|$$

$$= \sum_{I=1}^{4} 1.24\, N_{krI} \left[\frac{1}{\lambda}\right]_{\lambda_2}^{\lambda_1}$$

However, before the radiated photons reach the photo-cathode they pass through the glass window and are reflected by the internal side of the conical tube. The corresponding reflection and transmission factors have to be taken into account. Figure 5b and 5c illustrate these parameters, and table 3 summarizes the detailed factor in the range of wavelength where the P-M appears to be sensitive (fig. 5a).

Taking into account all these data, one can theoretically expect to have 0.20328 photoelectrons per proton.

REFERENCES

1. J. Litt, R. Meunier, Čerenkov counter technique in high-energy physics. Ann.Rev.Nucl.Sci. 23, 1-43 (1973).

2. G.W. Kaye, T.H. Laby, Longman, Tables of physical and chemical constants (1973).

3. For more information, see : Photo-multiplier Manual RCA (1970).

4. Philips Electron tubes data. Handbook, part 9 (1976).

5. CERN EP Division. PM supply type 4239, provisional specifications, Edition 29.3.1976.

6. CERN EP Division, PM supply control type 4240, provisional specifications, Edition 29.3.1976.

Table 1 : Refractive index of the investigated gasses

Gas	Refractive index	($p = 101325\ N/m^2$) ($t = 20^o\ C$)
Air	1.0002926	
CO_2	1.000451	
Ethylene	1.000696	
Neon	1.000067	
Argon	1.000281	
Helium	1.000036	

Table 2 : Refractive index and emission angle in the case of air as function of the wavelength

λ_{nm}	Refractive index	Θ deg.
350	1.0002850	1.341
400	1.0002817	1.333
450	1.0002796	1.328
500	1.0002781	1.324
550	1.0002771	1.322
600	1.0002763	1.320
650	1.0002758	1.319

Table 3 : Spectral ranges with their efficiencies

Range nm	P-M Spectral response mA/w	Window Transmission factor %	Reflective factor of aluminium %
390-420	80	70	90
420-450	80	80	90
450-550	60	90	90
550-600	25	90	90

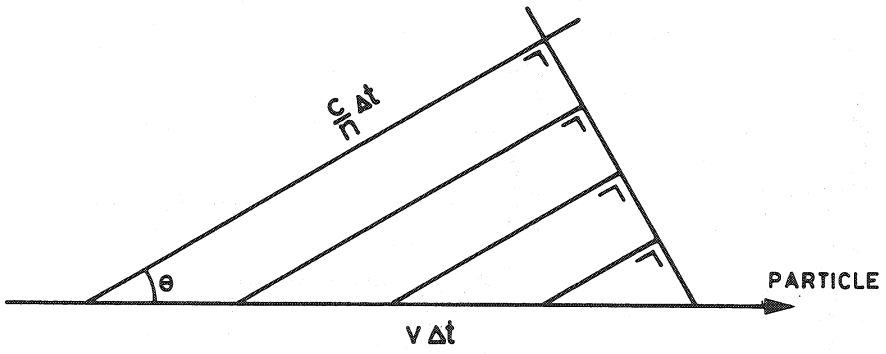

FIGURE 1

Wave front construction due to the passage of a charged particle with $v > \frac{c}{n}$

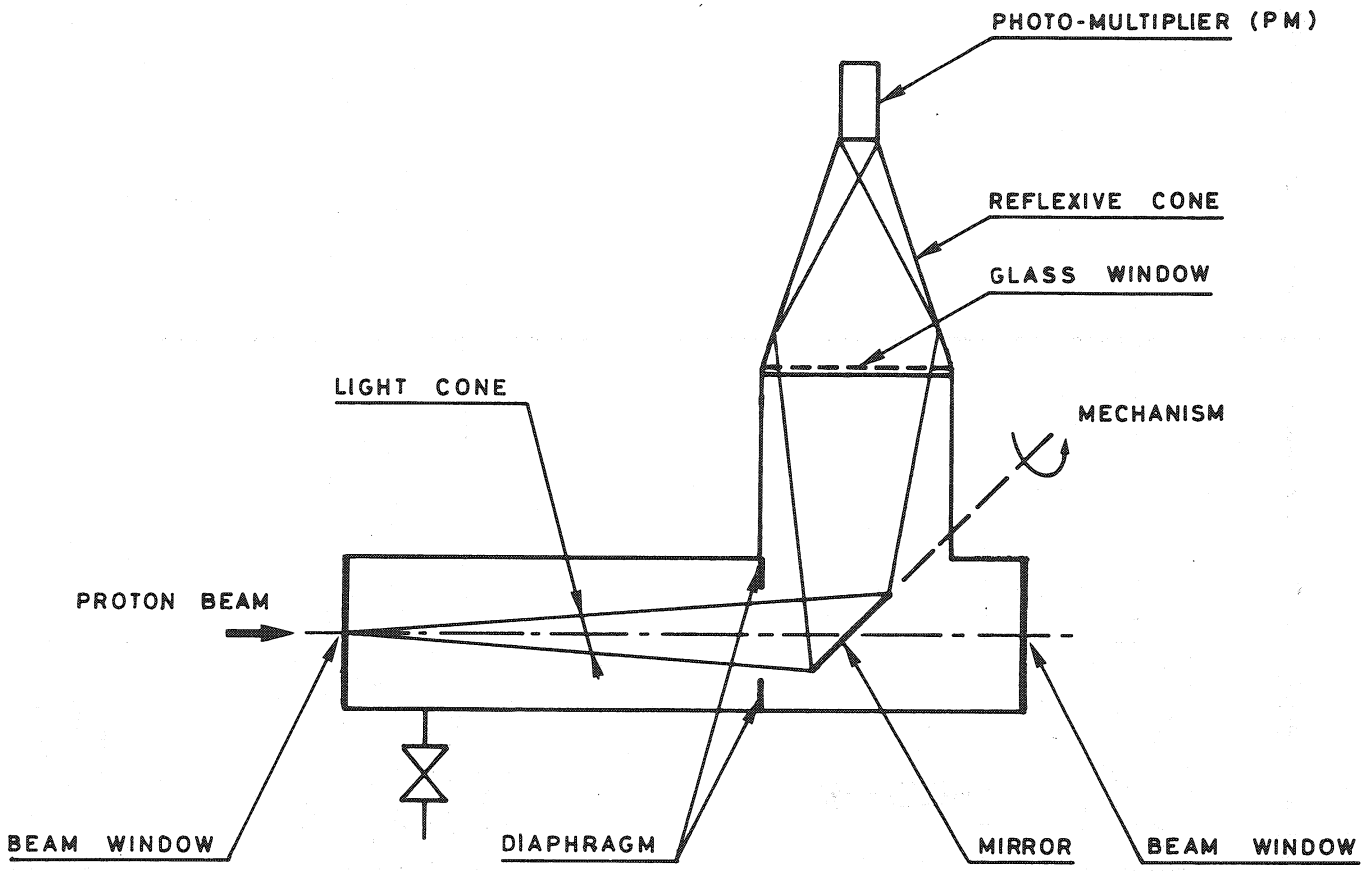

FIGURE 2

Detector configuration

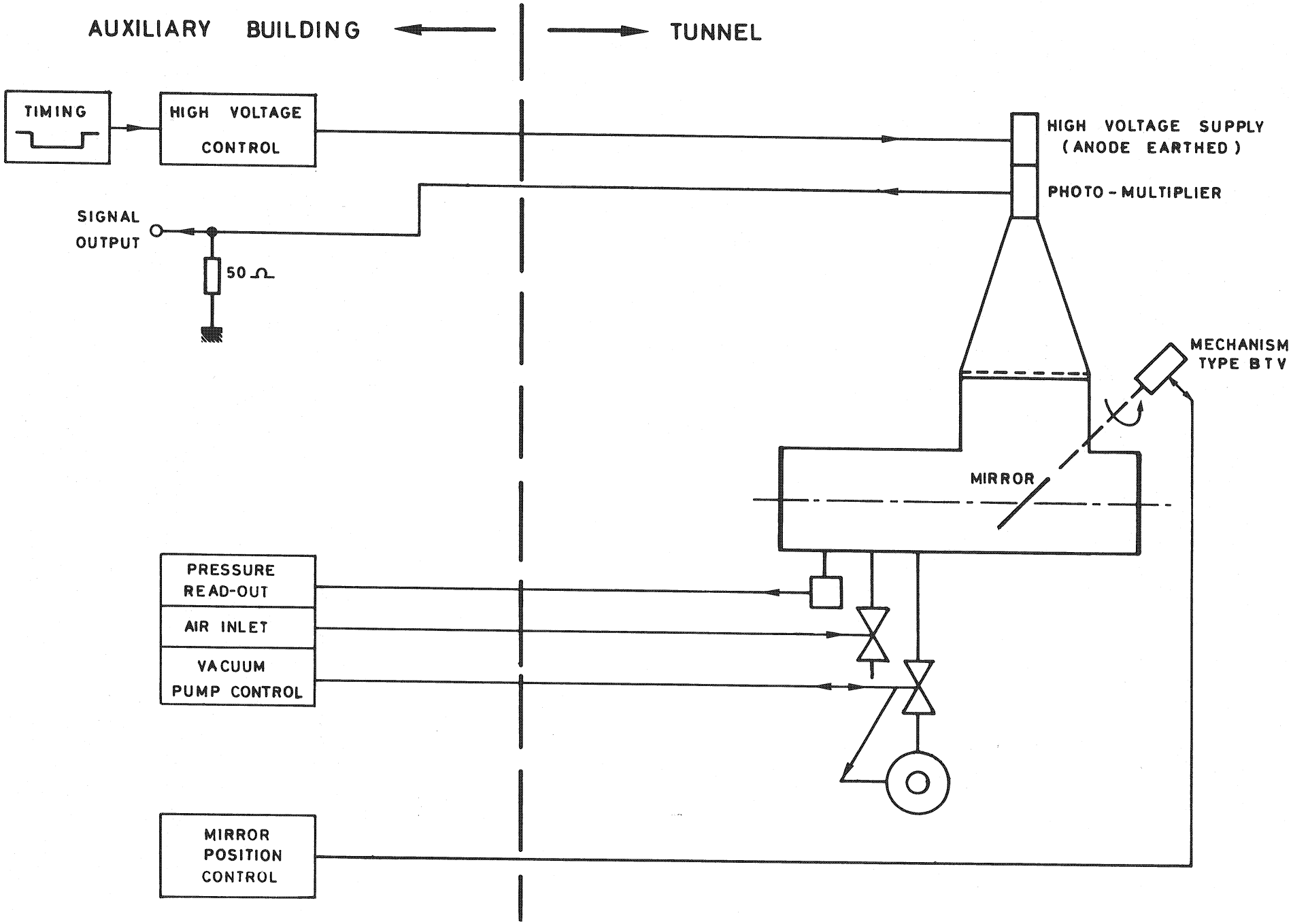

FIGURE 3 : Control of the detector

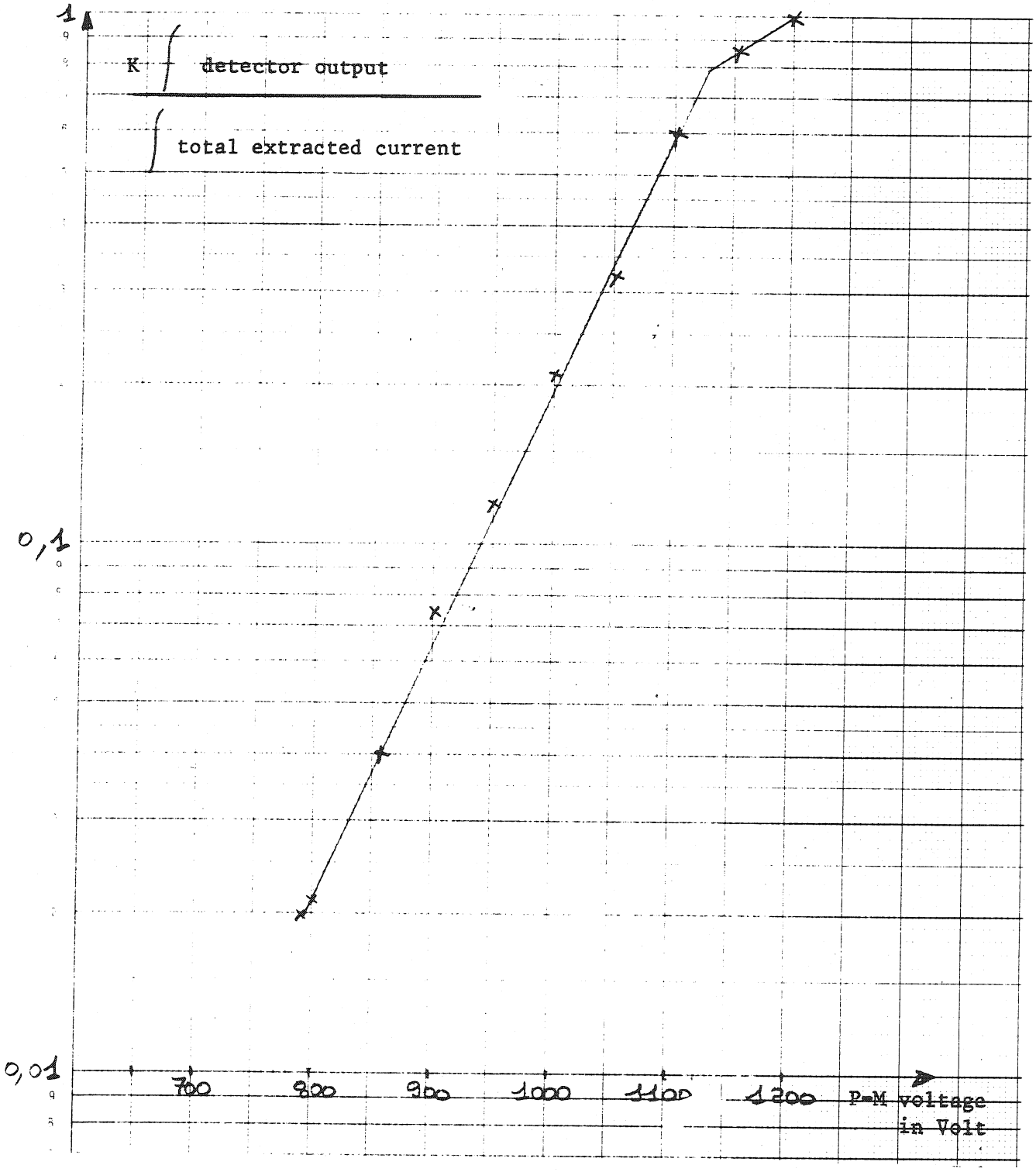

Fig. 4

Measurement of linearity

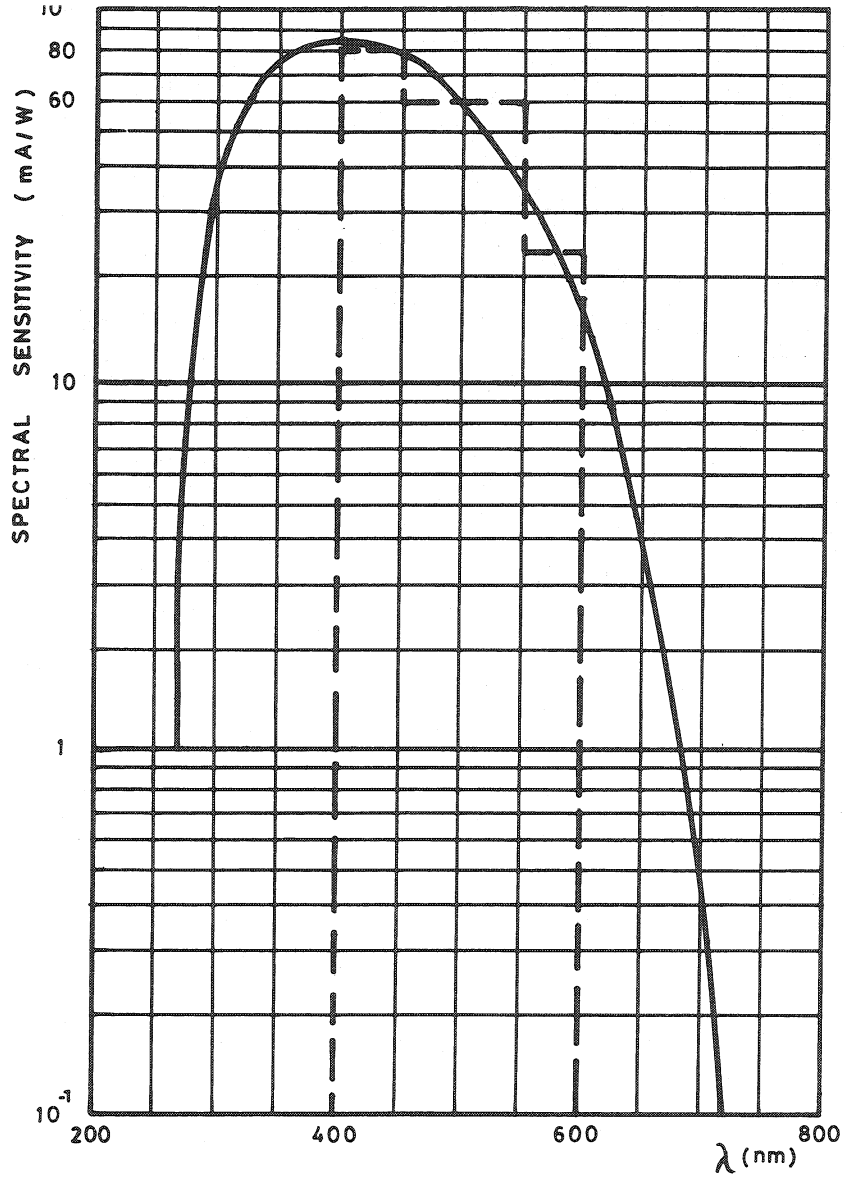

FIGURE 5a)

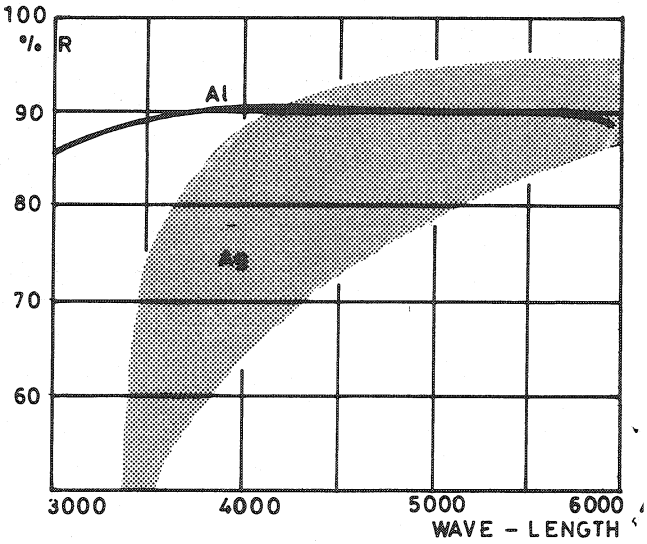

FIGURE 5b)

Reflection factor of Aluminium and Silver

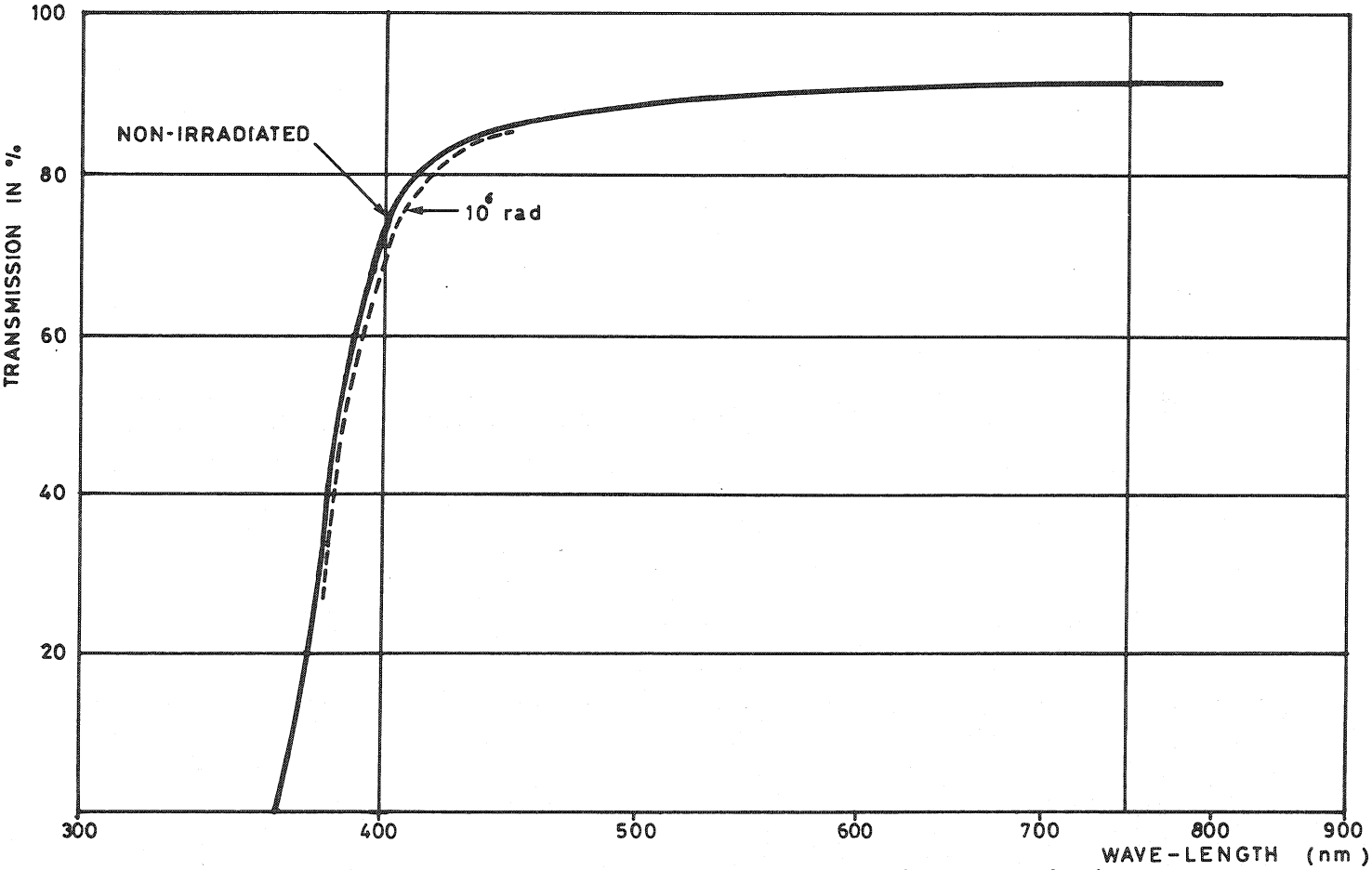

FIGURE 5c) Transmission curve of the glass window, before and after irradiation (ref : SCHOTT , MAINZ)

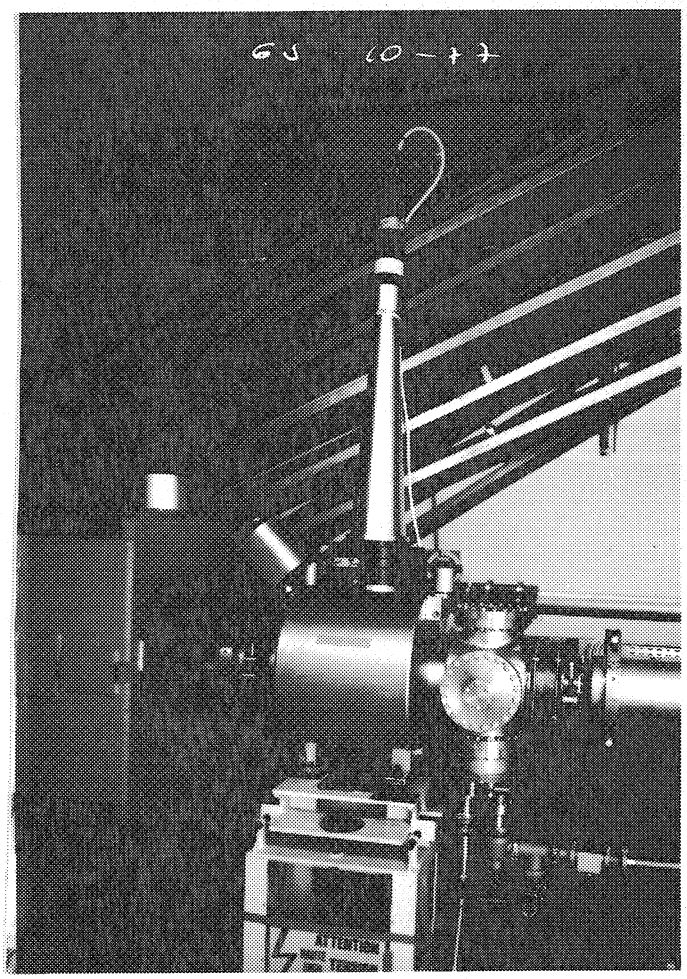

Photo 1 : The detector

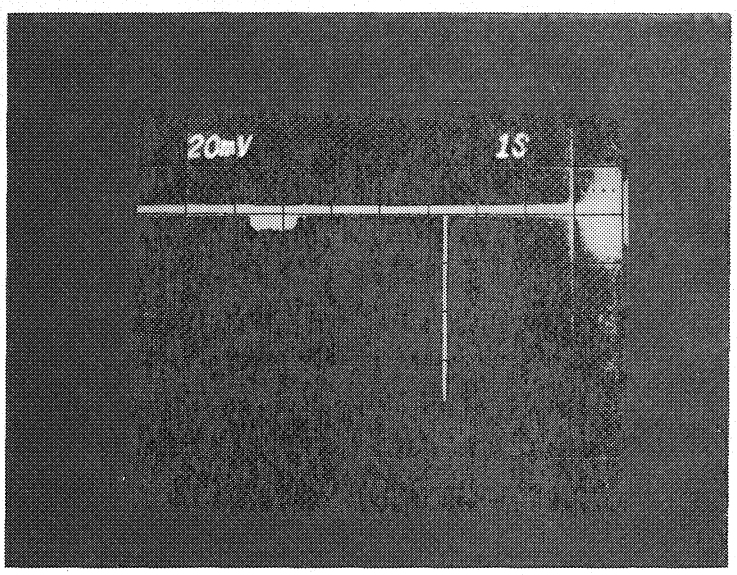

Photo 2

Photo 3

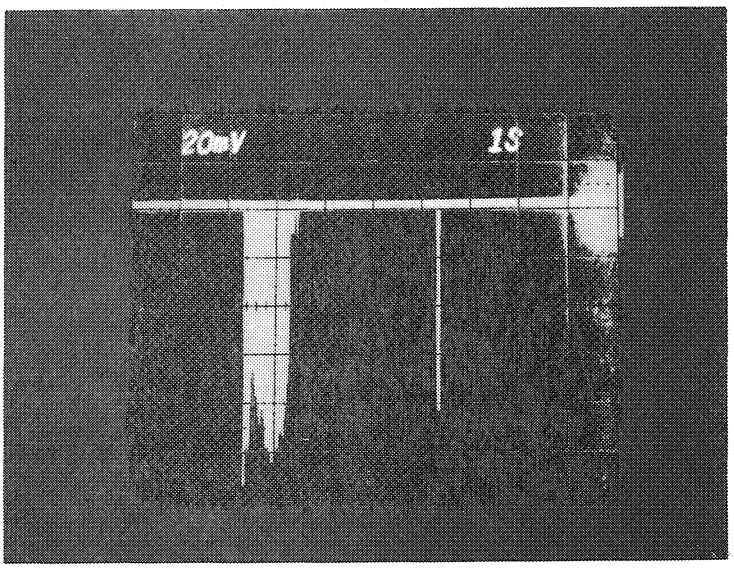

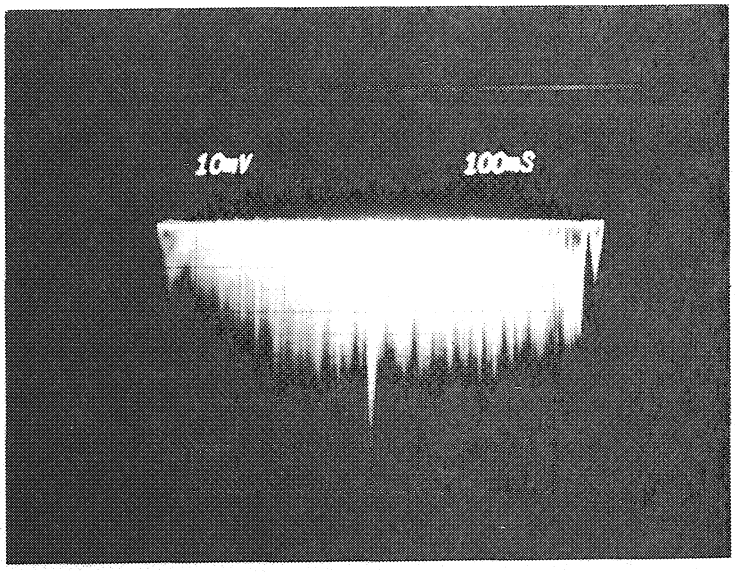

Photo 4

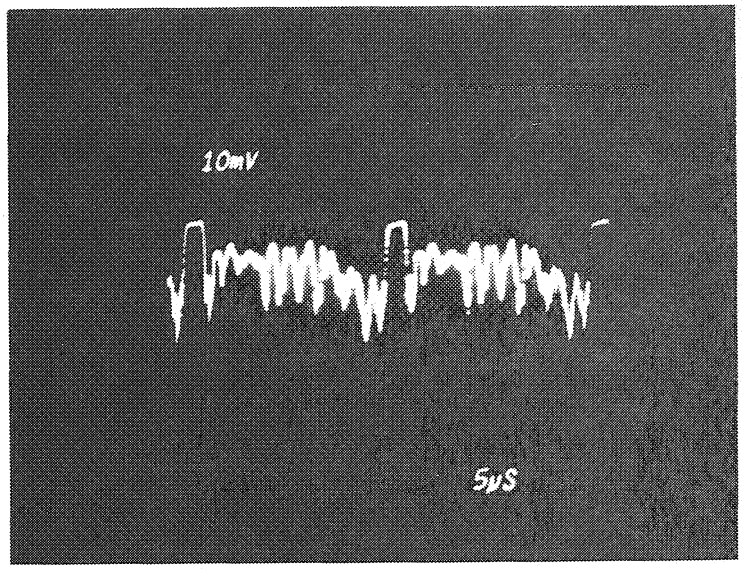

Photo 5

Photo 6

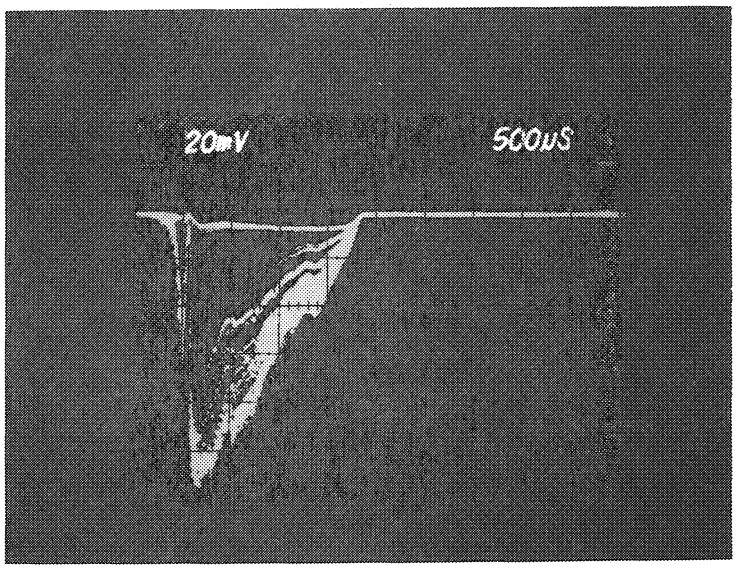

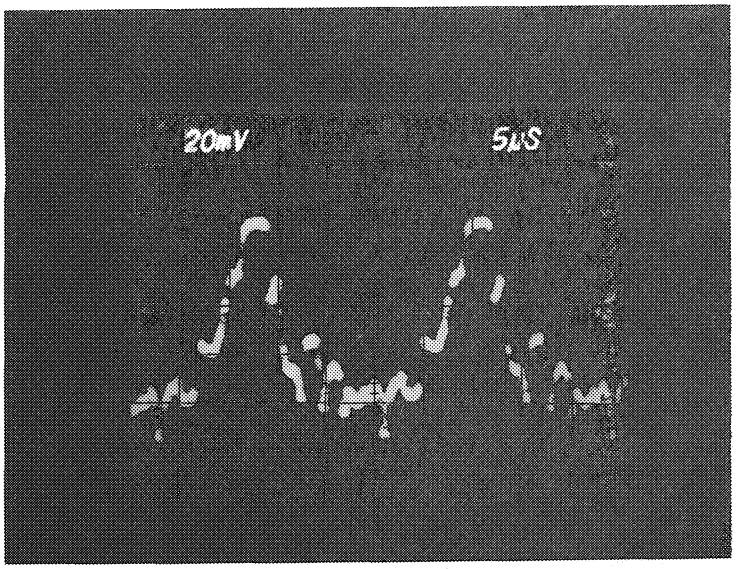

Photo 7

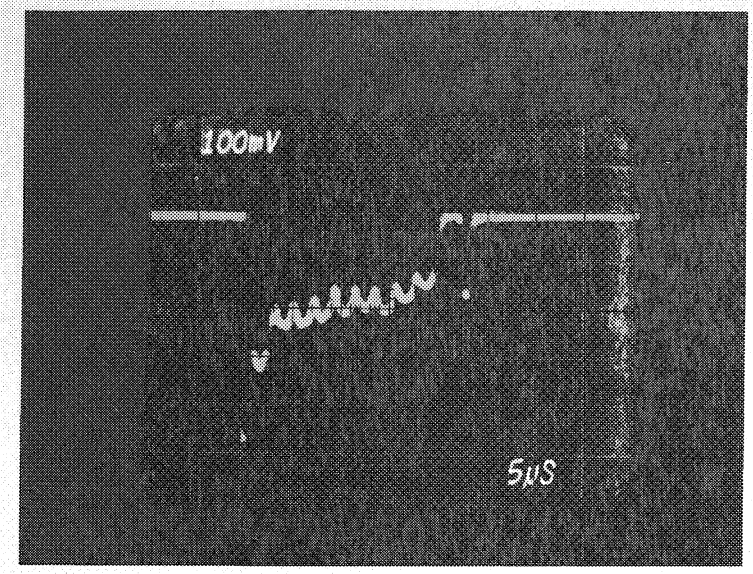

Photo 8

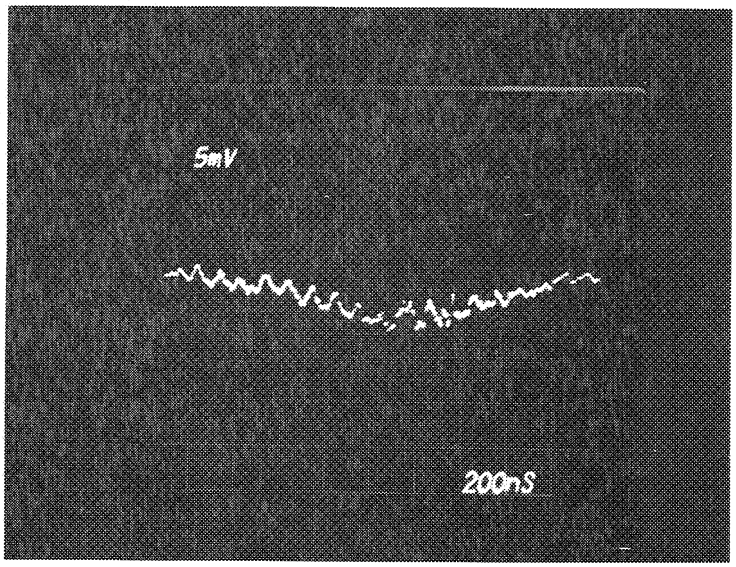

Photo 9